Spectrum Detection and Link Quality Assessment for Heterogeneous Shared Access Networks

Bin Li, Weisi Guo, *Senior Member, IEEE* Haijun Zhang, *Member, IEEE* Chenglin Zhao,
Shenghong Li, A. Nallanathan, *Fellow, IEEE*

Abstract—The persistent awareness of dynamic links quality is of critical importance to shared access systems, e.g. promoting sensing accuracy or even enabling seamless sharing, which remains yet as a challenging task. In this work, we consider the shared access in heterogeneous small-cells, which are likely to be the main infrastructure components by utilizing the carrier aggregation (CA) scheme, potentially combining both licensed and unlicensed bands. We suggest a promising sensing scheme, which permits the simultaneous assessment of multiple links quality when detecting vacant spectrum. We incorporate an additional objective of acquiring dynamic link state information (LSI) of multiple incumbent transmitters/receivers, and thereby structure spectrum sensing as a mixed classification and estimation (MCE) problem. The main challenge is that multiple channels may become similar with each other, and existing joint estimation schemes are unable to distinguish which incumbent is active and what its associated channel state is. To address this indistinguishable problem and alleviate the error propagation in recursive estimations, a novel *alternating Bernoulli filtering (ABF)* algorithm is proposed. By fully exploiting the group transitional behaviour of incumbents, a multiple-chains inference framework is developed. Numerical simulations validate our new scheme. Occupancy states of multiple incumbents can be identified accurately, by tracking their links quality and exploiting the underlying dynamics, which lays the foundation for more effective shared access.

Index Terms—Shared access, small-cell, link quality, mixed classification/estimation, alternating Bernoulli filtering

I. INTRODUCTION

THE NEXT-generation communication networks (e.g. 5G) will continue to pursue high spectral-efficiency techniques to meet the ever-increasing data demand, especially in dense urban scenarios [1], [2]. In recent years, advances in detection/estimation algorithms has enabled the spectrum shared accessing through real-time channel perception and intelligent system adaption. In the near future, seamless spectrum sharing is capable of alleviating the spectrum scarcity and may form the cornerstone of 5G communications [3], [4]. Already, spectrum sharing amongst non-contiguous bands is

Bin Li and Chenglin Zhao are with the School of Information and Communication Engineering (SICE), Beijing University of Posts and Telecommunications (BUPT), Beijing, 100876, China. (Email: stonebupt@gmail.com).

Weisi Guo is with School of Engineering, University of Warwick, West Midlands, CV47AL. (Email: Weisi.Guo@warwick.ac.uk)

Haijun Zhang is with University of Science and Technology Beijing, Beijing, China. (Email: dr.haijun.zhang@ieee.org)

Shenghong Li is with Department of Electronic Engineering, Shanghai Jiao-Tong University, Dongchuan Road, Shanghai 200240, China. (Email: shli@stju.edu.cn)

A. Nallanathan is with the Department of Informatics, King's College London, London, WC2R2LS, United Kingdom. (Email: nallanathan@ieee.org)

Manuscript received June 10, 2017.

a key component of License-Assisted-Access (LAA), which permits 4G small-cells to access unlicensed spectrum under the framework of LTE-Unlicensed (LTE-U). There is active interest from both the academic community and industrial practitioners to develop robust and fair spectrum sharing techniques based on the basic principle of listen-before-talk (LBT) [5], whilst also suppressing the mutual interference [6], [7]. To enable the aforementioned shared access capability, robust dynamic spectrum sharing (DSS) schemes would become essential for small-cells, which are likely to be the main infrastructure components in future networks by utilizing carrier aggregation (CA) schemes.

A. Shared Accessing

In principal, DSS is rooted on two main functionalities, i.e. *listen* to the radio environment, and then *talk* with adjustable transmission strategies [8]. The first action, known also as spectrum sensing [9], drives subsequent actions with the necessary knowledge of the radio environment. The second action, i.e. the adjustment to shared transmissions [10], [11], analyzes the current environment and takes action. It is readily supposed that the more information there is on dynamic wireless environments, the more freedom of adaption and the higher shared capacity can be achieved [12].

From this perspective, many existing DSS schemes that only sense the occupancy state of spectrum bands and make binary access decisions [13]–[15], will be insufficient to the emerging shared access, where there may be a high spatial-temporal traffic demand intensity. As such, evaluating the quality of parallel radio links will be definitely of crucial importance to shared access systems. In this paper, except for the spectrum occupancy state, we define the link quality in a broad sense to include various related link state information (LSI) between incumbents (or primary user - PU) and shared user (or secondary user - SU), such as: dynamic fading channels, PU's mobile locations [18], transmission parameters of PU [16], [17], and so on.

1) Spectrum Sensing: In spectrum sensing, the detection accuracy can be improved by suppressing the information uncertainty due to unknown channels. Current methods include marginalising the uncertain knowledge (e.g. channel fading) [21], [22], as well as estimating the dynamic LSI from PU's emitter to SU. The latter can be accomplished by jointly estimating the related link qualities when detecting the occupancy state of spectrum. In previous research by the authors [12], [18], a *Bayesian estimation framework* has been

designed to acquire various LSI (e.g. fading channels and PU's locations), which is essentially abstracted as one joint detection and estimation problem [12], [25].

2) Spectrum Access: In spectrum access stage, the links quality assessment that accompanies the sensing process provides a broad view on external wireless environments, which is of great promise to the seamless spectrum sharing and the improvement of shared capacity, e.g. enabling intelligent power control or spatial multiplexing in heterogeneous small cells. For example, the crosstalk channel gain (from PU's receiver to SU) can be utilized to adjust SU's emission power when conducting shared transmissions, e.g. in underlay D2D applications. Despite these appealing prospects, most existing sensing schemes fail to support flexible shared access applications [19], [20].

B. Summary of Challenges

To sum up, there are three formidable challenges when applying existing schemes to heterogeneous shared access.

First, existing sensing methods, i.e., energy detection (ED) [21], matched-filter detection [23], covariance matrix method [36], and cyclo-stationary feature detection [24], would implement reliable sensing in various practical applications [19], [20]. When it comes to simultaneous spectrum detection and channel quality assessment, most of them would become inapplicable. As such a new signal processing task involves several challenges, e.g., the disappearance of likelihood (e.g. when PU is silent), the coupling interaction between detection and parameter estimation, as well as the resulting error propagations. As such, their sensing performance will be limited and the related link state information can be hardly obtained.

Second, whilst the dynamical channel gain from a PU transmitter could be estimated by another joint estimation method [12], [18], [25], due to the *asymmetric* links and the hidden terminal problem (HTP), the estimated channel quality (with regard to an incumbent transmitter) cannot fully characterize the cross-interference to its receiver.

Third, the estimation of multiple channel gains becomes challenging to a time division duplexing (TDD) network. To be specific, spectrum sensing with simultaneous channel assessment, in the context of multiple TDD incumbents, has the new structure of a more complicated problem–**mixed classification and estimation** (MCE). I.e., the sensing procedure is supposed not only to identify which single incumbent is emitting signal, but also to estimate what its associated link state is in. When fading gains of two links become comparable (as two channels evolve independently along time), the likelihood densities of two possible active links are almost the same. Thus, one may detect the channel is occupied, but can hardly judge which one single TDD PU is emitting signals. And, the inevitable error detection will affect the recursive inference.

As far as we are aware, there is no theoretical framework reported in the literature to cope with this MCE problem. Thus, our new algorithm is designed to detect multiple active primary devices and also estimate related link quality, i.e. fading gains.

C. Proposed Solutions and Methodological Contributions

To solve the encountered MCE problem, we derive a new sensing scheme for heterogeneous small cell scenarios, enabling the joint assessment of dynamic links quality between multiple incumbent transmitters/receivers and SUs. The main contributions of this work are listed as follows.

1. We formulate a general dynamic state-space model (DSM) for the considered TDD scenario [26], in which only one incumbent/PU may be active in each time slot. We assume the links quality change dynamically with time. All J ($J \geq 2$) PUs' emission states and the fading channels of PU-SU links are treated as *hidden* states.

2. We design a sequential estimation algorithm, with which the links quality can be simultaneously estimated when identifying the single active PU. A new ABF algorithm is developed, which, in contrast to classical *Bernoulli filtering (BF)* schemes, is able to track the trajectories of multiple PUs' states as well as their associated channel states. To accomplish this, we proposed a multi-chain estimation concept, by exploiting the group transitional behaviors of multiple incumbents as well as the historical inference results. In order to deal with the indistinguishable problem that is peculiar to our MCE formulation, a novel post-processing scheme is further designed. By adjusting the estimated posterior densities of multi-chains according to the dominance of their inference outputs, the error propagation in recursive estimations would be alleviated.

3. We evaluate both the detection/classification and estimation performance of the ABF scheme. It is demonstrated that, compared with existing BF algorithms, our new ABF algorithm will significantly reduce the estimation mean square error (MSE) of dynamic fading channels. The sensing accuracy of multiple PUs can be significantly improved when compared to other example counterpart algorithms [12], [18]. The acquired links quality, as additional knowledge on environments, enable the further enhancement of overall shared access network performance in heterogeneous small cell environments.

The rest of the detailed work is structured as follows. In Section II, a dynamic state-space model in the context of multiple TDD PUs is formulated. In Section III, the novel Bayesian estimation scheme is designed, and a novel ABF is developed to track multiple fading channels and PUs' states, whereby a competition and enhancement mechanism is also integrated. In Section IV, numerical analysis is provided. Finally, we conclude the study in Section V.

II. SYSTEM MODEL

We consider an indoor small cell network and assume multiple PUs of a small cell communication with each other on specific spectrum band [7], by using a TDD mode [26]. For the considered scenarios [27], the TDD mode allows for the flexible UL/DL timeslot allocation. It is capable of matching uplink/downlink resources to real-time traffic demand, and thereby maximizing the system throughput [28], e.g. in the Planto cell architecture recently proposed by DOCOMO. As illustrated in Fig. 1, other shared users (e.g. a D2D link) can convey direct transmissions via the shared access ecosystem. In such cases, the LBT scheme can be adopted to control
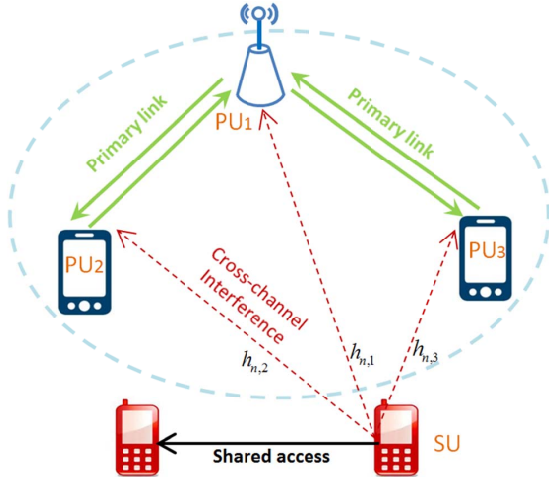
Fig. 1. Shared access and transmission between heterogeneous D2D devices and an indoor TDD small-cell network.

the mutual interference and thereby achieve the harmonious sharing, by imposing the minimal coordination on two heterogeneous systems.

At each time n, at most one PU would be active (e.g. the j_nth), whilst the others stay inactive or receive information. The shared D2D devices are authorized to access the spectrum without significantly affecting PUs. To be specific, the device is allowed to transmit signals either with no emission constraints (when all PUs are inactive, i.e. overlay sharing), or by configuring a low emission power (when only one PU is active, i.e. underlay sharing). Thus, the cornerstone of intelligent shared access in heterogeneous small cells is the accurate acquisition of both multiple emission states and the dynamic link quality. Note that, this work focus on the time-varying channel gains, while the other types link quality will be considered in future by extending our proposed scheme in a straightforward way.

A. Dynamic State-space Model

A dynamic state space approach is used to characterise spectrum sensing process with simultaneous link quality assessment, i.e.

$$\mathbf{s}_n = S(\mathbf{s}_{n-1}), \tag{1}$$
$$\mathbf{h}_n = H(\mathbf{h}_{n-1}), \tag{2}$$
$$y_n = Y(\mathbf{h}_n, \mathbf{s}_n, w_{n,m}). \tag{3}$$

The first two *dynamic* equations Eqs. (1)-(2) describe the transitions of PUs' unknown states $\mathbf{s}_n$ and the evolution of associated PU-SU channels $\mathbf{h}_n$, respectively. The *measurement* equation Eq. (3) specifies the coupling relation between the observation y_n and two hidden states, i.e. $\mathbf{s}_n$ and $\mathbf{h}_n$.

B. Multiple PUs' States

In the analysis, $s_{n,j} \in \{0,1\}$ denotes the jth PU's state at the nth discrete time, where "0" accounts for inactive and "1" for active state. For clarity, we denote total J PU's states with one $J \times 1$ vector $\mathbf{s}_n \triangleq \{s_{n,j}\} \in \mathcal{S} \subset \mathbb{Z}^J$. As far as a TDD

mode is concerned, for any time n we will have $||\mathbf{s}||_2 \leq 1$. Note that, the all-inactive state is denoted by $s_0 = s_{n,0}$ ($s_{n,0}$ means $s_{n,j}$=0 for any j), whilst the active state is $s_1 = s_{n,1} \oplus s_{n,2} \oplus \cdots \oplus s_{n,J}$ (i.e. there exist only one active PU with $s_{n,j} = 1$).

The evolutions of multiple TDD PUs' states depend on previous states, as in Eq. (1), which are modelled as the 1st order discrete-states Markov chain (DSFC) [30]. For the considered $(J + 1)$-state system, the transitional probability matrix (TPM) is:

$$\mathbf{P} = \begin{bmatrix} p_{0\to0} & p_{0\to1} & \cdots & p_{0\to J} \\ p_{1\to0} & p_{1\to1} & \cdots & p_{1\to J} \\ \vdots & \vdots & \ddots & \vdots \\ p_{J\to0} & p_{J\to1} & \cdots & p_{J\to J} \end{bmatrix}.$$

where each transitional probability is defined as $p_{i\to j} \triangleq \Pr\{s_{n,j}|s_{n-1,i}\}$ ($i, j = 0, 1, \cdots, J$).

Among all probabilistic transitions, the event that the jth PU stays active at both the previous time $(n - 1)$ and the current time n is referred as to "*survival*" [18], and the jth survival probability is $p_{n,j}^s \triangleq \Pr\{s_{n,j} = 1|s_{n-1,j} = 1\}$. The jth PU may switch to the inactive state with a probability $(1 - p_{n,j}^s)$ in the time n. Meanwhile, the event that the jth PU is inactive in previous slot $n-1$ and switches into active at the time n is mentioned as "*birth*", characterized by the birth probability:

$$p_{n,j}^b \triangleq \Pr\{s_{n,j} = 1|s_{n-1,j} = 0\},$$
$$= \sum_{k\in\mathcal{J},k\neq j} \Pr\{s_{n,j} = 1|s_{n-1,j} = 0, s_{n-1,k}\},$$
$$= \Pr\{s_{n,j} = 1|s_{n-1,j} = 0, s_{n-1,k\neq j} = 0\}$$
$$+ \sum_{k\in\mathcal{J},k\neq j} \Pr\{s_{n,j} = 1|s_{n-1,j} = 0, s_{n-1,k} = 1\},$$

where $\mathcal{J} \triangleq \{1, 2, \cdots, J\}$. At time n, the jth PU may stay also inactive with a probability of $1 - p_{n,j}^b$.

Based on the above elaboration, the dynamic state function $S(\cdot): \mathbb{Z}^J \mapsto \mathbb{Z}^J$ is inexplicit, defined by a group of stochastic transitional densities, i.e.,

$$\Pr\{S(\mathbf{s}_{n-1}) = \mathbf{s}_n\} = \Pr\{\mathbf{s}_{n-1}|\mathbf{s}_n\}, \mathbf{s}_n \in \mathcal{S}. \tag{4}$$

C. Dynamic Channels

The time dynamics of channel gain $\mathbf{h}_n = \{h_{n,j}\} \in \mathcal{H}^J \subseteq \mathbb{R}^J$ is modelled as the finite-states Markov chain (FSMC) [31]. Without the lose of generality, we consider the fading states of J PU-SU links change independently. The dynamic function $H(\cdot) : \mathbb{R}^J \mapsto \mathbb{R}^J$, which characterizes the evolution of link gains, is thereby determined by a group of transitional probabilities, i.e.

$$\Pr\{H(\mathbf{h}_{n-1}) = \mathbf{h}_n\} = \Pr\{\mathbf{h}_{n-1}|\mathbf{h}_n\},$$
$$= \prod_{j=1}^{J} \Pr\{h_{n-1,j}|h_{n,j}\}. \tag{5}$$

Here, each fading state $h_{n,j}$ takes values from a finite set $\mathcal{H}_j \triangleq \{\mathsf{H}_{j,k}, \ k = 1, 2, \cdots, K\}$, and each single transitional term in Eq. (5) is given by:

$$\Theta_{k_1\to k_2, j} \triangleq \Pr\{H(h_{n-1,j}) = h_{n,j}\}, \tag{6}$$
$$= \Pr\{h_{n,j} = \mathsf{H}_{k_2,j}|h_{n-1,j} = \mathsf{H}_{k_1,j}\},$$

where each representative fading state $\mathsf{H}_{k,j}$ is determined by the fading distribution $f(h_j)$ (e.g. Rayleigh fading) and the division bounds of amplitudes [32], [33], i.e., $\mathsf{H}_{k,j} = \int_{\mathfrak{D}_{k,j}} h_{n,j} f(h_{n,j}) dh_{n,j} / \int_{v_{k,j}}^{v_{k+1,j}} f(h_{n,j}) dh_{n,j}$. That is to say, the kth dividing bound will restrict fading amplitude to the region $\mathfrak{D}_{k,j} = (v_{k-1,j}, v_{k,j}]$ $(v_{k,j} \geqslant 0)$. Here, the equiprobable partition rule is adopted, and we have $\pi_{k,j} = \int_{\mathfrak{D}_{k,j}} f(h_j) dh_j = 1/K$. In this case, the division bound is derived via $v_{k,j} = \left[-2\sigma_j^2 \ln(1 - k/K)\right]^{1/2}$ [31].

The duration of a sensing-transmission frame would be T_F=20$\sim$100ms. On the other hand, the typical mobile speed in non-vehicular applications is around 0.08$\sim$0.09km/h [34], i.e. the root mean square (RMS) Doppler spread is about 0.414Hz (e.g. the carrier frequency is f_c=2.4GHz) and the channel coherent time T_c is 800$\sim$1000 ms. That means, the channel gain $\mathbf{h}_n$ will keep temporarily invariant in $L = \lfloor T_c/T_F \rfloor = 8 \sim 50$ successive slots, whilst the channel states may transit at a switching time $n' = \lfloor n/L \rfloor$, while keeping invariant at the others times. Thus, our analysis focuses on slow-varying fading channels. Furthermore, a first-order FSMC is concerned, which has been proven to be sufficient for slow-varying environments [31]–[33]. I.e., the TPM $\boldsymbol{\Theta}_{K \times K, j} \triangleq \{\Theta_{k \to k', j}, k, k' \in \{0, 1, \cdots, K - 1\}\}$ tends to be a *tri-diagonal* matrix. That means, at each switching time n', the fading state can only transit to itself or its 1-step neighbour states, i.e., we have $\Theta_{k \to k', j} = 0$ for $|k - k'| > 1$.

D. Observations

Given the little coordination imposed on two shared systems, the non-coherent energy observation is used. The energy observation $y_n \in \mathcal{Y} \subset \mathbb{R}^1$ will be measured via $Y(\cdot) : \mathbb{R}^M \mapsto \mathbb{R}^1$, which is specified by:

$$y_n = \sum_{j=1}^J \sum_{m=1}^M \delta(s_{n,j} - 1) \times [h_{n,j} d_{n,j}(m) + w_{n,j}(m)]^2, \quad (7)$$

$$= \begin{cases} \sum_{m=1}^M [h_{n,j} d_{n,j}(m) + w_{n,j}(m)]^2, & s_{n,k} = 1, \ s_{n,k \neq j} = 0, \\ \sum_{m=1}^M w_{n,1}^2(m), & s_{n,j} = 0. \end{cases}$$

In measurement process, the noise samples $w_n(m) \in \mathbb{R}^1$ $(m = 1, 2, \cdots, M)$ is zero-mean additive white Gaussian noise (AWGN) with a variance of σ_w^2, i.e., $w_n(m) \sim \mathcal{N}(0, \sigma_w^2)$. The samples size is M. Since only one PU will be active at each time n, a Direchlet function $\delta(x)$ is used to indicate which single PU is emitting signals. The unknown signals from the jth PU is denoted as $d_{n,j}(m) = b_{n,j}(m) \times p(m)$, where $\{b_{n,j}(m)\}$ accounts for PU's signals and $p(m)$ represents a specific pulse-shaping response. For simplicity, the real-valued binary phase shift keying (BPSK) signal is considered by the analysis, e.g., $b_{n,j}(m) \in \mathcal{B} = \{+\sigma_b, -\sigma_b\}$, with the variance $E_j = \mathbb{E}_{\mathcal{B}}\{d_{n,j}(m)^2\} = \sigma_b^2$. As far as the non-coherent observation is concerned, however, the generalisation to other modulated signals would be straightforward.

According to the central limits theorem (CLT), the likelihoods of observation can be approximated by the Gaussian distributions (when M is lager). Conditioned on the fading gain $\mathbf{h}_n$ and PUs' states $\mathbf{s}_n$, the likelihood densities will be:

$$\varphi(y_n|s_{n,j}) = \mathcal{N}\{M\sigma_w^2, 4M\sigma_w^4\}, \quad (8)$$
$$\varphi(y_n|h_{n,j}, s_{n,j}) = \mathcal{N}\left\{ME_j h_{n,j}^2 \sigma_w^2, ME_j h_{n,j}^2 \sigma_w^2 + 4M\sigma_w^4\right\}. \quad (9)$$

III. SPECTRUM SENSING WITH CHANNEL QUALITIES ASSESSMENT

Our new objective is then to jointly detect multiple PU's state and acquiring the associated link quality. Different from traditional schemes based on Neyman-Pearson (NP) criterion to solved a two-hypothesis test (THT) problem [14], [36], here the maximum *a posteriori* (MAP) criterion is suggested. I.e., the unknown PUs' states, accompanying multiple dynamic channels, are estimated via:

$$(\hat{\mathbf{h}}_n, \hat{\mathbf{s}}_n) = \arg \max_{\mathbf{h}_n \in \mathcal{H}^J, \mathbf{s}_n \in \mathcal{S}} p(\mathbf{h}_{1:n}, \mathbf{s}_{1:n}|y_{1:n}), \quad (10)$$

where $\mathbf{s}_{1:n} \triangleq \{\mathbf{s}_1, \cdots, \mathbf{s}_n\}$ denotes the trajectory of PUs' states until the nth slot, while $\mathbf{h}_{1:n}$ and $y_{1:n}$ are two trajectories of channels and observations.

A. Multiple-Chain RFS

In order to characterize the MCE problem with multiple TDD PUs and dynamical links quality, a *multi-chain* random finite set (MC-RFS) model is formulated. Here, an RFS refers to a special random set, whereby the number of elements (active PU) as well as their associated states (fading channels) changes with time.

In our case, the number of elements of single RFS $\boldsymbol{\mathcal{F}}_n$ [37], known as the RFS cardinality and denoted by $d_n = |\boldsymbol{\mathcal{F}}_n|$, is a Bernoulli variable following $\zeta(d_n) = \Pr\{|\boldsymbol{\mathcal{F}}_n| = d_n\}$, $d_n \in \{0, 1\}$ [38], [39]. I.e., when the cardinality of is d_n=0, there will be no active PU at the time n. In contrast to a classical RFS [18], [40], even if the cardinality of this multi-chain RFS is d_n=1 (i.e. one single PU is active), however we cannot know which single PU is active currently and what its associated link state is.

A finite set statistics (FISST) PDF $p(\boldsymbol{\mathcal{F}}_n)$ is of importance to the statistical inference of RFS, and here we adopt Mahler's approach to define it [37], [40], i.e.

$$p(\boldsymbol{\mathcal{F}}_n = \{\mathbf{f}_1, \mathbf{f}_2, \cdots, \mathbf{f}_d\}) = n! \zeta(d_n) p(\{\mathbf{f}_1, \mathbf{f}_2, \cdots, \mathbf{f}_d\}), \quad (11)$$

where $\mathbf{f}_d$ is the unknown state vector associated with the dth element, and $p(\{\mathbf{f}_1, \mathbf{f}_2, \cdots, \mathbf{f}_d\})$ is a group of joint distributions. Subsequently, we give three densities of interest to $\boldsymbol{\mathcal{F}}_n$.

1) Cardinality Distribution: As mentioned, the cardinality of MC-RFS indicates whether there involves one active PU. In our case, the cardinality density $\zeta(d_n)$ is:

$$\zeta(d) = \begin{cases} 1 - \sum_{j=1}^J q_{n,j}, & \text{if } |\boldsymbol{\mathcal{F}}_n| = 0 \text{ or } \boldsymbol{\mathcal{F}}_n = \varnothing, \quad (12a) \\ \sum_{j=1}^J q_{n,j}, & \text{if } |\boldsymbol{\mathcal{F}}_n| = 1 \text{ or } \boldsymbol{\mathcal{F}}_n = \{h_{n,j}\}. \quad (12b) \end{cases}$$

From Eq. (12), $\boldsymbol{\mathcal{F}}_n$ will be either *empty* with a probability $1 - q_n$ or have one *single* active PU with the probability q_n, where $q_n \triangleq \sum_{j=1}^{J} q_{n,j}$. Here, $q_{n,j}$ denotes the existence probability of the jth chain (or the jth PU). Thus, a crux arises in the multiple incumbents scenarios, i.e., even if the cardinality is $d_n = 1$ at time n, any single PUs would be active.

2) RFS PDF: The FISST PDF $p(\boldsymbol{\mathcal{F}}_n)$ depends on a cardinality distribution, i.e. $\zeta(d_n)$, and the spatial distribution of fading channels, i.e. $p(\mathbf{h}_n)$, which is given by:

$$p(\boldsymbol{\mathcal{F}}_n) = \begin{cases} 1 - \sum_{j=1}^{J} q_{n,j}, & \text{if } \boldsymbol{\mathcal{F}}_n = \varnothing, \quad (13a) \\ \sum_{j=1}^{J} q_{n,j} \cdot p(h_{n,j}), & \text{if } \boldsymbol{\mathcal{F}}_n = \{h_{n,j}\}. \quad (13b) \end{cases}$$

For $d_n > 1$, we have $p(\boldsymbol{\mathcal{F}}_n)=0$. Note that, here $\int_{\boldsymbol{\mathcal{F}}} p(\boldsymbol{\mathcal{F}}_n)\delta\boldsymbol{\mathcal{F}}_n$ represents the set integration on $\boldsymbol{\mathcal{F}}$, rather than the random distribution marginalisation.

3) Transitional Densities: In line with our new MC-RFS, the *a priori* transitional probabilities are given by:

$$\phi_{n|n-1}(\boldsymbol{\mathcal{F}}_n|\varnothing)$$
$$= \begin{cases} p_{0\to0}, & \text{if } \boldsymbol{\mathcal{F}}_n = \varnothing, \quad (14a) \\ \sum_{j=1}^{J} p_{0\to j} \times b_{n|n-1,j}(h_{n,j}), & \text{if } \boldsymbol{\mathcal{F}}_n = \{h_{n,j}\}, \quad (14b) \end{cases}$$

and

$$\phi_{n|n-1}(\boldsymbol{\mathcal{F}}_n|\{h_{n,j}\}) = \begin{cases} \sum_{j=1}^{J} q_{n-1,j} \cdot p_{j\to0}, & \text{if } \boldsymbol{\mathcal{F}}_n = \varnothing, (15a) \\ \sum_{j=1}^{J} q_{n-1,j} \cdot \Delta_{n,j}, & \text{else}, \quad (15b) \end{cases}$$

respectively, where each transitional term of channels is

$$\Delta_{n,j} = p_{j\to j} \cdot \Theta_{n|n-1,j}(h_{n,j}|h_{n-1,j})$$
$$+ \sum_{j'\in\mathcal{J},j'\neq j} p_{j\to j'} \times b_{n|n-1,k}(h_{n,j'}). \quad (16)$$

Here, $b_{n|n-1,j}(h_{n,j}) \triangleq \Pr\{h_{n,j}|q_{n-1,j} = 0\}$ represent the birth densities, which define a group of initial distributions of channel states $\{h_{n,j}\}$ (when the jth PU is birthed at time n). The design of birth distributions will be discussed shortly.

B. Sequential MAP

A two-stage scheme, i.e. predicting and updating, can be suggested to track both multiple PUs' emission states and dynamic channel states, i.e.

$$p_{n|n-1}(\boldsymbol{\mathcal{F}}_n|y_{1:n-1}) =$$
$$\int_{\boldsymbol{\mathcal{F}}_{n-1}} \phi_{n|n-1}(\boldsymbol{\mathcal{F}}_n|\boldsymbol{\mathcal{F}}_{n-1}) \times p_{n-1|n-1}(\boldsymbol{\mathcal{F}}_{n-1}|y_{1:n-1})d\boldsymbol{\mathcal{F}}_{n-1},$$
$$(17)$$

$$p_{n|n}(\boldsymbol{\mathcal{F}}_n|y\mathbf{z}_{1:n}) = \frac{\varphi_n(y_n|\boldsymbol{\mathcal{F}}_n)p_{n|n-1}(\boldsymbol{\mathcal{F}}_n|y_{1:n-1})}{\int_{\boldsymbol{\mathcal{F}}_n} \varphi_n(y_n|\boldsymbol{\mathcal{F}}_n)p_{n|n-1}(\boldsymbol{\mathcal{F}}_n|y_{1:n-1})d\boldsymbol{\mathcal{F}}_n}.$$
$$(18)$$

Note that, as analyzed, the particular indistinguishable problem will render existing joint estimation schemes (e.g. in [12], [18]) invalid. Given that the fading channels of J PU-SU links will change independently, in the following we designed an two-phases MC-RFS estimation framework.

Firstly, J chains are employed to separately estimate each PU's states and associated fading channels. Each chain recursively obtains the corresponding posterior PDF $p_{n|n,j}(\boldsymbol{\mathcal{F}}_n|y_{1:n})$ based on observations y_n. From Eq. (13), two posteriy densities will be of great interest in determining $p_{n|n,j}(\boldsymbol{\mathcal{F}}_n|y_{1:n})$ [12], i.e. the jth posterior existence density

$$q_{n|n,j} \triangleq \Pr\left(|\boldsymbol{\mathcal{F}}_n| = 1, s_{n,j} = 1|y_{1:n}\right), \; j = 1, 2, \quad (19)$$

and *a posteriori* spatial PDF of link state $\{h_{n,j}\}$, i.e.,

$$f_{n|n,j}\left(\boldsymbol{\mathcal{F}}_n = \{h_{n,j}\}\right) \triangleq p(h_{n,j} = \mathsf{H}_{k,j}), \; j = 1, 2. \quad (20)$$

Secondly, relying on the overall outputs from J chains, i.e. J posterior existence densities $q_{n|n,j}$ and spatial densities $f_{n|n,j}(\{h_{n,j}\}|y_{1:n})$, a competition process will be implemented. A final decision on which single PU is active most probably will be reached (in the case of H_1). At the same time, its corresponding posterior existence density will be enhanced, whilst the posterior existence densities of the others (i.e. inactive PUs) are suppressed.

C. Alternating Bernoulli Filtering

In order to estimate two related densities in Eqs. (19) and (20), a novel ABF algorithm is designed. It fully exploits the group transitional behaviour of J PUs as well as the historical inference results of J chains, which can alleviate the error propagation in recursive estimations.

*1) **Prediction Stage**:* First, given the initial value $q_{0|0,j}$, the predicted existence density $q_{n|n-1,j}$ will be recursively derived (see `Appendix A`), i.e.,

$$q_{n|n-1,j} = \Pr(s_{n,j} = 1|y_{1:n})$$
$$= \underbrace{p_{n,j}^b \times \prod_{j'=1}^{J}(1 - q_{n-1|n-1,j'})}_{\text{birth term}}$$
$$+ \underbrace{p_{j\to j} \times q_{n-1|n-1,j} \cdot \prod_{j'\in\mathcal{J},j'\neq j}(1 - q_{n-1|n-1,j'})}_{\text{survival term}}$$
$$+ \underbrace{\sum_{j'\neq j} p_{j'\to j} \times q_{n-1|n-1,j'} \cdot \prod_{j_0\in\mathcal{J},j_0\neq j',j_0\neq j}(1 - q_{n-1|n-1,j_0})}_{\text{transition term}}.$$
$$(21)$$

From the above equation, we observe that the predicted existence density, i.e. $q_{n|n-1,j}$, consists of three following independent components. A well-defined schematic structure of calculating the predicted existence densities is shown also by Fig. 2.

(1) The first *birth* component indicates that the jth PU enters into an active state at time n, on the condition that there is no active PUs at the previous time $(n - 1)$. Thus, it is related with the probability $\Pr\{s_{n-1,j} = 0, s_{n-1,j'\neq j} = 0\} = \prod_{j=1}^{J}(1 - q_{n-1|n-1,j})$. Recall that $q_{n-1|n-1,j}$ denotes
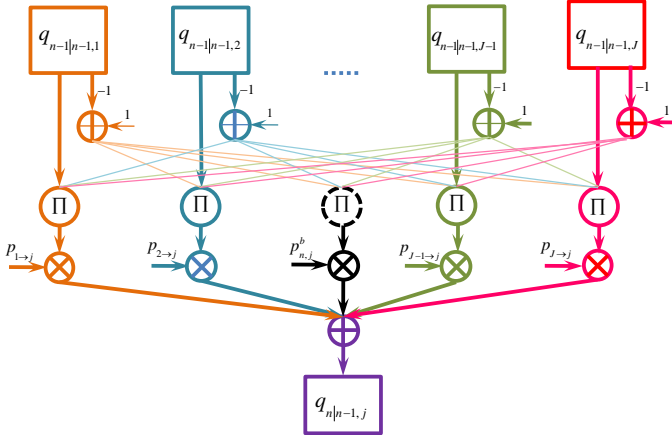
Fig. 2. A schematic structure of generating the predicted existence density from the group transitional property and previous inference results.

the existence probability of the jth PU at time $(n-1)$, $(1 - q_{n-1|n-1,j})$ gives the absence/inactive probability.

(2) The second *survival* component suggests the jth PU remains active at both current time n and previous time $(n-1)$. Here, $\Pr\{s_{n-1,j} = 1, s_{n-1,j'\neq j} = 0\} = q_{n-1|n-1,j} \cdot \prod_{j'\in\mathcal{J}, j'\neq j}(1 - q_{n-1|n-1,j'})$ accounts for the probability that the jth PU is active at time $(n-1)$, whilst the others stay inactive. Note that, for the concerned TDD mode, here we have $\Pr\{s_{n-1,j} = 1\} = \Pr\{s_{n-1,j} = 1, s_{n-1,j'\neq j} = 0\}$.

(3) The third *transitional* component corresponds to another case, i.e., the j'th $(j' \neq j)$ PU is active at time $(n-1)$, whilst the other jth PU switches to the active state at time n. Here, total $(J-1)$ possible transitions are involved. Such a transition term can be regarded also as one special birth component.

Second, the predicted spatial density $f_{n|n-1,j}$ is derived recursively (see Appendix B). In line with the predicted existence density, it involves also three components, i.e.,

$$f_{n|n-1,j}(h_{n,j}|y_{1:n-1}) = p^b_{n|n-1,j}(h_{n,j}|y_{1:n-1}) + p^s_{n|n-1,j}(h_{n,j}|y_{1:n-1}) + p^t_{n|n-1,j}(h_{n,j}|y_{1:n-1}). \quad (22)$$

(1) The first *birth* component is structured as:

$$p^b_{n|n-1,j}(\{h_{n,j}\}|y_{1:n-1}) = b_{n|n-1,j}(h_{n,j}) \times \frac{p_{0\to j} \cdot \prod_{j'=1}(1 - q_{n-1|n-1,j'})}{q_{n|n-1,j}}, \quad (23)$$

which characterises the birth process of the jth PU, on the condition that there is no active PU at previous time $n-1$ (with a probability $p_{0\to j} \cdot \prod_{j'=1}(1 - q_{n-1|n-1,j'})$). Once the jth PU is birthed at time n, the *a priori* spatial density $b_{n|n-1,j}(h_{n,j})$ is exploited to predict the distribution of its link state (which will be elaborated in Appendix D).

(2) The second *survival* component is given by:

$$p^s_{n|n-1,j}(\{h_{n,j}\}|y_{1:n-1})$$
$$= \frac{p^s_{n,j} \times q_{n-1|n-1,j'} \prod_{j'\neq j}(1 - q_{n-1|n-1,j'})}{q_{n|n-1,j}}$$
$$\times \int_{\mathcal{H}_j} \Theta_{n|n-1,j}(h_{n,j}|h_{n-1,j}) \cdot f_{n-1|n-1,j}(h_{n-1,j})dh_{n-1,j}, \quad (24)$$

which is related with the one-step predicted density $\int_{\mathcal{H}_j} \Theta_{n|n-1,j}(h_{n,j}|h_{n-1,j}) \cdot f_{n-1|n-1,j}(h_{n-1,j})dh_{n-1,j}$, given the jth PU remains active at both time $n-1$ and n. As discussed, the conditional density of survival is related with $p^s_{n,j} \times q_{n-1|n-1,j'} \prod_{j'\neq j}(1 - q_{n-1|n-1,j'})$.

(3) The third *transition* component is given by:

$$p^t_{n|n-1,j}(\{h_{n,j}\}|y_{1:n-1}) = b_{n|n-1,j}(h_{n,j}) \times$$
$$\frac{\sum_{j'\neq j} p_{j'\to j} q_{n-1|n-1,j'} \cdot \prod_{j'\neq j}(1 - q_{n-1|n-1,j'})}{q_{n|n-1,j}}, \quad (25)$$

which, as another special kind of birth component, is related also with the birth density.

It should be noted from Eq. (22) that, involving three complementary components, the predicted spatial density $f_{n|n-1,j}(h_{n,j})$ remains dominantly different from the classical BF process [39], [40]. In particular, from Eq. (22), the birthed component is now contributed by two terms, i.e. the birth of the jth PU or the transition from another j'th $(j' \neq j)$ PU.

2) Update Stage: Both the predicted existence density and the predicted spatial density are then updated on the new observation y_n, see Eq. (26) at the bottom of the Page and Eq. (27).

$$f_{n|n,j}(h_{n,j}) = \frac{r_{n,j}(y_n|h_{n,j}) \times f_{n|n-1,j}(h_{n,j})}{\int_{\mathcal{H}_j} r_{n,j}(y_n|h_{n,j}) \times f_{n|n-1,j}(h_{n,j})dh_{n,j}}. \quad (27)$$

Here, the term $r_{n,j}(y_n|\{h_{n,j}\})$ is referred to as the likelihood ratio (see Appendix C).

With the predict and update process, total J posterior existence densities $\{q_{n|n,j}\}$ and spatial densities $\{f_{n|n,j}(h_{n,j})\}$ can be derived. It is noted that, from the above derivations, a classical BF scheme can be regarded as one *special case* of the ABF, where the number of TDD PUs is $J=1$ [12].

Relying on the posterior existence densities $\{q_{n|n,j}\}$ and spatial densities $\{f_{n|n,j}(h_{n,j})\}$, the active PU will be identified in the case of H_1, and its associated link state will be estimated. To be specific, after configuring a threshold γ, the jth PU's state is estimated via:

$$\hat{s}_{n,j} = \begin{cases} 1, & \text{if } q_{n|n,j} > \gamma, \quad (28a) \\ 0, & \text{if } q_{n|n,j} \leq \gamma. \quad (28b) \end{cases}$$

$$q_{n|n,j} = \frac{q_{n|n-1,j} \times \int_{\mathcal{H}_j} r_{n,j}(y_n|h_{n,j}) \cdot f_{n|n-1,j}(h_{n,j})dh_{n,j}}{(1 - q_{n|n-1,j}) + q_{n|n-1,j} \times \int_{\mathcal{H}_j} r_{n,j}(y_n|h_{n,j}) \cdot f_{n|n-1,j}(h_{n,j})dh_{n,j}}. \quad (26)$$

In practice, the threshold γ will be configured to 0.5, as far as a Bayesian rule is concerned. Meanwhile, the jth channel state is acquired via:

$$\hat{h}_{n,j} = \arg \max_{h_{n,j} \in \mathcal{H}_j} f_{n|n,j}(h_{n,j}). \tag{29}$$

Based on the above ABF scheme, both the channel state (i.e. $\hat{s}_{n,j}$) as well as the associated fading channel $\hat{h}_{n,j}$ can be derived via derived posterior densities (**Challenge 1**). As such, for the TDD network, the HTP problem would be addressed, i.e., the shared user can even access the occupied channel (by PU1), by limiting its averaged interference to possible primacy receivers (PU1 or PU3) via the estimated cross-channel fading gains (i.e. $\hat{h}_{n,2}$ and $\hat{h}_{n,3}$) (**Challenge 2**).

D. Competition and Enhancement

Due to comparable channel gains, more than one PUs' existence probabilities $q_{n|n,j}$ would surpass a threshold γ at time n. In other words, we cannot distinguish which incumbent (or PU) is actually active with existing joint estimation schemes [12], [18], no mention to the quality assessment of related multiple links. To cope with such an indistinguishable problem, a novel **competition and enhancement mechanism** (CEM) is further designed.

The underlying conception will be relatively intuitive. First, the single PU (i.e. the j_nth PU) that is most probably emitting signals at time n (if d_n=1) is identified, and its existence density $q_{n|n,j_n}$ is enhanced. Second, the existence density of the remaining probably inactive PUs, i.e. $q_{n|n,j \neq j_n}$, are suppressed. That is, the output posterior densities of each RFS chains will be adjusted automatically.

1) Competition Stage: The index of the most probably active PU is firstly identified via Eq. (30), which is denoted by $j_n \in \mathcal{J}_n$, i.e.,

$$j_n = \arg \max_{j \in \mathcal{J}_n}\{q_{n|n,j} \times f_{n|n,j}(h_{n,j})\}, \tag{30}$$
$$\mathcal{J}_n = \{j|q_{n|n,j} > \gamma\}.$$

As in eq. (30), we consider the j_nth PU with the maximum FISST PDF, i.e. $\max\{q_{n|n,j} \times f_{n|n,j}(h_{n,j})\}$, is most probably emitting signals at time n when $|\mathcal{J}_n| > 1$. Accordingly, we further rectify the detection results, by configuring the j_nth active indicator to 1 and the other indicators to 0, i.e.,

$$Q_{n,j_n} = 1, Q_{n,j' \neq j_n} = 0. \tag{31}$$

At the same time, its associated channel state will be determined directly via Eq. (29). In contrast, the channel states of the other j'th PU ($j' \neq j_n$), i.e. $h_{n,j'}$ ($j' \neq j_n$), will be estimated via the following Eq. (32). That means, at each switching time n, the channel state of the j'th inactive PU will be predicted via *a priori* transitional density.

$$\hat{h}_{n,j'} = \arg \max_{|k_1-k_2|\leq 1} \Pr\left\{h_{n,j'} = \mathsf{H}_{k_2,j'}|\hat{h}_{n-1,j'} = \mathsf{H}_{k_1,j'}\right\}. \tag{32}$$

2) Enhancement Stage: After identifying the j_nth active PU (when at least one $q_{n|n,j}$ larger than γ), then its posterior existence density will be enhanced, i.e.,

$$q_{n|n,j_n} = p_{j_n}(n) \times p_{\max}(y_n|h_{n,j_n}, s_{n,j_n} = 1). \tag{33}$$

Here, it is easy to understand that the prior component $p_{j_n}(n)$ is associated with both the j_nth existence density of time $(n-1)$ (i.e. Q_{n-1,j_n}) and the *a priori* transitional densities. From the Eqs. (34)-(35), $p_{j_n}(n)$ can be viewed as a dynamical prior probability of two cases at time n, i.e. survival ($Q_{n-1,j_n} = 1$) or birth ($Q_{n-1,j_n} = 0$). Meanwhile, the likelihood term $p_{\max}(y_n|h_{n,j_n}, s_{n,j_n} = 1)$ is given by Eq. (36), which actually accounts for the maximum conditional posterior density of the j_nth channel states, i.e.,

$$p_{\max}(y_n|h_{n,j_n}, s_{n,j_n} = 1)$$
$$= \max_{h_{n,j} \in \mathcal{H}_j} \varphi(y_n|h_{n,j}, s_{n,j}) \times \Theta(h_{n,j_n}|\hat{h}_{n-1,j_n}). \tag{36}$$

At the same time of enhancing the j_nth posterior density, the posterior densities of the other remaining $(J-1)$ inactive PUs will be suppressed, i.e.

$$q_{n|n,j'} = p_{j'}(n) \times p(y_n|s_n = 0), \tag{37}$$

where the prior terms are determined via Eqs. (38)-(39) at the bottom of the Page. A normalized process will be applied then. For other possible cases, Eqs. (33)-(36) will be only used to update the active PU whose posterior existence probability is larger than a threshold γ. In this way, the encountered MCE problem is solved, and the error propagation can be alleviated (**Challenge 3**).

E. Implementation and Extension

Given that the implementation of our proposed ABF algorithm involves complex and non-analytical densities, a particle filtering (PF) scheme is utilised to numerically estimate the

$$p_{j_n}(n) = \begin{cases} q_{n-1|n-1,j_n} \cdot \prod_{j' \neq j_n} (1 - q_{n-1|n-1,j'}) \times p_{j_n \to j_n}, & \text{if } Q_{n-1,j_n} = 1, \tag{34} \\ \prod_{j \in \mathcal{J}} (1 - q_{n-1|n-1,j}) \cdot p_{0 \to j_n} + \sum_{j' \neq j_n} q_{n-1|n-1,j'} \cdot \prod_{j_0 \neq j'} (1 - q_{n-1|n-1,j_0}) \times p_{j' \to j_n}, & \text{if } Q_{n-1,j_n} = 0. \tag{35} \end{cases}$$

$$p_{j'}(n) = \begin{cases} 1 - q_{n-1|n-1,j'} \cdot \prod_{j_0 \neq j'} (1 - q_{n-1|n-1,j_0}) \times p_{j' \to j'}, & \text{if } Q_{n-1,j'} = 1, \tag{38} \\ 1 - \prod_{j \in \mathcal{J}} (1 - q_{n-1|n-1,j}) \cdot p_{0 \to j'} - \sum_{j \neq j'} q_{n-1|n-1,j} \cdot \prod_{j_0 \neq j} (1 - q_{n-1|n-1,j_0}) \times p_{j \to j'}, & \text{if } Q_{n-1,j'} = 0. \tag{39} \end{cases}$$

intractable densities, via $I = (N + B)$ simulated discrete particles [41] (and the details are given in `Appendix D`).

To maximise the functioning of our ABF scheme, two refinement operations, i.e. clamping and accumulating, are used. First, once the same channel state $h_{n,j}$ has been estimated for R (e.g. R=4) times within the static length L (in the case of H_1), then the channel estimation will be clamped to $h_{n,j}$. Second, the observations of previous slots within the statical period are accumulated (when PU's signal is detected), which is used at current time n to further improve the estimation accuracy.

The complexity of the ABF algorithm is measured by $O[JK_1(N + B)\vartheta + M^2]$ multiplications. Here, M^2 accounts for the complexity in calculating the summed energy; K_1 is the number of feasible transitional states of dynamical channels, which equals to 3 for the 1st-order DSMC; ϑ accounts for the computation of related likelihood densities; $(N + B)$ accounts for the used discrete particles in PF. It is seen that the implementation complexity of the proposed scheme is higher than that of ED, which has a complexity of $O(M^2)$.

Notice that, the generalization of our designed algorithm to other link state information, e.g. mobile locations, is also possible. To be specific, we may adopt a random walking model [18] (or other mobility models) to reformulate the dynamic state-space model in Eq. (1)-(3). Then, the association of unknown channel state $s_{n,j}$ and PUs mobile locations (i.e. $[lx_{n,j}, ly_{n,j}]$) to the summed energy $y(n)$, as well as the likelihoods in Eqs. (8)-(9), can be determined. Thus, the recursive estimation can be implemented by our proposed ABF algorithm. Due to the limited budget, the emphasis of following analysis will be put on dynamics channel fading.

IV. NUMERICAL SIMULATIONS

This section is devoted to numerical simulations, and the sensing accuracy of multiple TDD PUs as well as the channel estimation MSE will be evaluated. To do so, we adopt two performance metrics in the following analysis. The first performance metric P_D, which jointly considers the detection reliability of each PU, is designed to evaluate not only the occupancy state (H_0 or H_1, or p_f and p_d), but also to determine which single PU is active at the current time. It has been suggested that this compound performance metric will be of great importance, in terms of maximising the utilisation of spectrum [12], [43]. The second metric, i.e. the estimation MSE of fading channels, is used to evaluate the accuracy of link quality assessment.

$$P_D = \mathbb{E}\left\{\sum_{j=1}^{J} \Pr(s_{n,j}) \times \Pr\{Q_{n,j} = s_{n,j}|s_{n,j}\}\right\}, \quad (43)$$

$$\text{MSE}_j \triangleq \frac{1}{N} \times \mathbb{E}\left\{\sum_{n=1}^{N} |\hat{h}_{n,j} - h_{n,j}|^2 / |h_{n,j}|^2\right\}. \quad (44)$$

1) Different Numbers J: First, the influence from different numbers of multiple TDD PUs on the classification/estimation performance of our ABF algorithm will be studied. In the simulations, the sample size is $M = 200$ and the particles size is $I = N + B = 200$ ($N = 100$ and $B = 100$). For dynamic
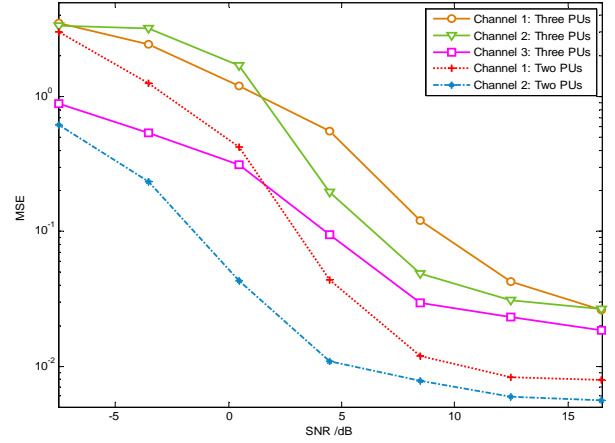

Fig. 3. Sensing performance of the designed scheme in the context of different static fading length.
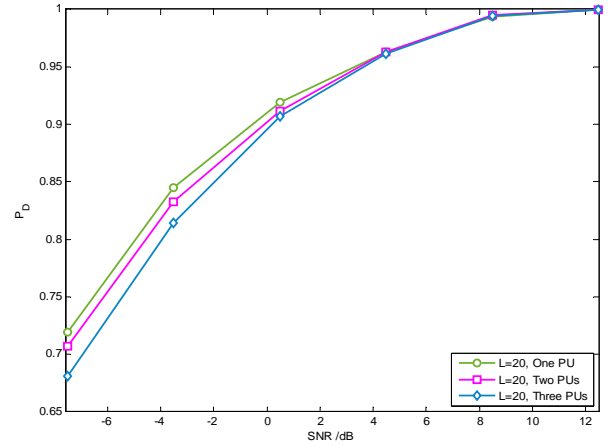

Fig. 4. MSE performance of the estimation fading channels in the context of different static length.

FSMC channels, the representative number of discrete states is K=7, and the static fading length is L=20. For the case of two TDD PUs (i.e. J=2), the fading variances are set to σ_1^2=0.1 and σ_2^2=0.15, respectively. A statistical TPM of PUs' states is:

$$\mathbf{P} = \begin{bmatrix} 0.5 & 0.2 & 0.3 \\ 0.2 & 0.3 & 0.5 \\ 0.3 & 0.5 & 0.2 \end{bmatrix}. \quad (45)$$

For the case of J=3, the fading variances are set to σ_1^2=0.1, σ_2^2=0.15 and σ_3^2=0.18, respectively. The statistical TPM of multiple PUs' states is:

$$\mathbf{P} = \begin{bmatrix} 0.3 & 0.1 & 0.2 & 0.4 \\ 0.2 & 0.3 & 0.3 & 0.2 \\ 0.3 & 0.4 & 0.2 & 0.1 \\ 0.2 & 0.2 & 0.3 & 0.3 \end{bmatrix}. \quad (46)$$

In Fig. 3, the numerical MSE performances under different numbers of TDD PUs are plotted. Without the loss of generality, we consider two typical normalized Doppler shifts, i.e. $f_D T_c$=0.02 and 0.05 (L=20 and 50), as in refs. [31]–[33]. Note that, other configurations of a static length L can be also applicable. It is found that, by fully utilizing the group
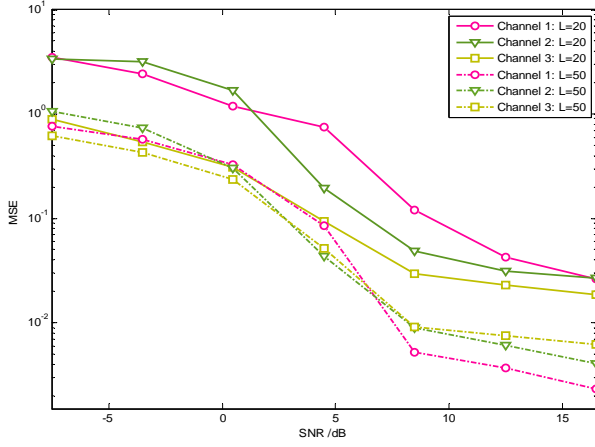
Fig. 5. MSE performance of the estimation fading channels in the context of different sample size.

Fig. 7. MSE performance (*Left*) and detection accuracy (*Right*) in the presence of inaccurate TPM, J=3, M=200 and L=16.
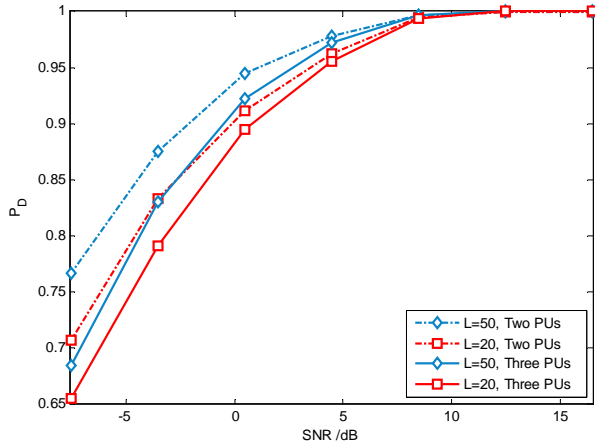

Fig. 6. MSE performance of the estimation fading channels in homogeneous and inhomogeneous fading variances.

transitional information of J PUs, the new ABF algorithm can cope with the indistinguishable problem. Recall in our new scheme, despite total J separate chains, all historical inference results (i.e., J posterior densities of time $(n-1)$) have been exploited by each RFS chain, when estimating unknown states of time n (as illustrated by Fig. 2). Besides, the competition and enhancement scheme is specially designed to mitigate the miss-classification effects, which may be aroused by the comparable channel gains. As a consequence, it indeed suppresses the error propagation in recursive estimation. Even so, we note from Fig. 3 that when the total number of TDD PUs is increased from J=2 to J=3, the estimation MSE of dynamic channels will be degraded accordingly. Taking the 1st PU-SU channel for example, the MSE will be increased from 1×10^{-3} to 6×10^{-3}, indicating the new ABF scheme can only alleviate but not avoid the indistinguishable problem.

From the numerical result in Fig. 4, the similar observation will be made to the sensing performance under different TDD PUs. It is seen that the probability of right detection (i.e. P_D) in the case of J=3 will be slightly inferior to that of J=2, due to the aforementioned indistinguishable problem. As the
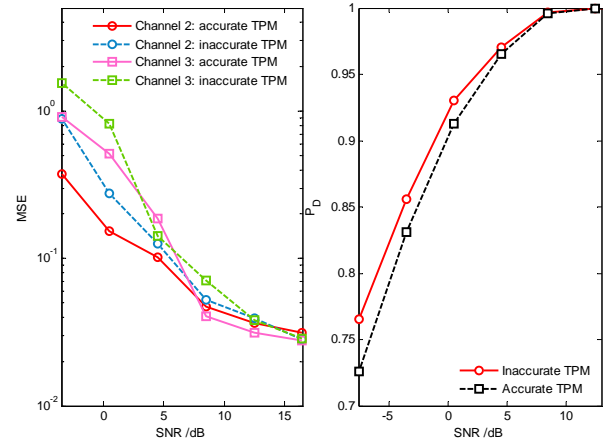
numbers of TDD PUs J increases ($J > 3$), the classification set $\{1, 2, \cdots, J\}$ will be enlarged, leading to the degraded classification performance due to the exacerbated mutual influence. Thus, the accuracy of channel quality assessment will be degraded as in Fig. 3, and the sensing performance will also be affected. Compared with the case of $J = 1$, a rough detection gain of $1 \sim 1.5$dB will be lost when $J = 3$ PUs need to be sensed. Besides, due to the degraded performance and less chance of vacant channel, we focus on small numbers of TDD PUs in the analysis.

2) Static Fading Length: Then, we investigate the effect on the channel tracking performance with different static length L. In the simulation, we assume J=3 TDD PUs. The sample size M is configured to 200. As demonstrated by Fig. 5, the channel estimation MSE will be reduced significantly, as the static length L increases from 20 to 50. From the numerical results, the MSE of channel assessments with L=20 will be ranged from $1.5 \sim 2.6 \times 10^{-2}$, when the SNR is 16.5dB. While for L=50, the channel estimation MSE will be about $2.2 \sim 6.1 \times 10^{-3}$. I.e., the slow-varying channel allows for the more adequate observation accumulation and thereby renders the likelihood density more accurate, leading to the improved estimation performance.

Meanwhile, the accuracy of spectrum sensing can be also improved by the larger static length L. From Fig. 6, compared with the fast-varying fading channel (e.g. $L = 20$), a rough detection gain of 2dB can be obtained when the slow-varying channel (e.g. $L = 50$) is concerned and the number of TDD PUs is configured to $J = 3$. Similar results will be observed in Fig. 6, where the sensing performance of $J = 2$ TDD PUs under different static length L are presented.

3) Influence of inaccurate TPM: In the absence of *a priori* TPM, a feasible way is to estimate related transitional probabilities, for example, directly using the methods in ref. [44], [45], which were designed to extract such statistic information of a hidden Markov process. On the other hand, our scheme is also relatively robust to such required prior information. In the following, we further challenged our ABF algorithm in the presence of inaccurate TPM. I.e., we used the TPM in
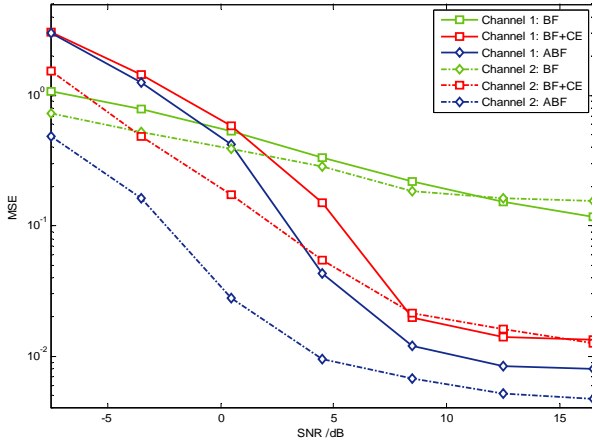
Fig. 8. MSE performance of channel estimation with different fading variances. Here, CE is the abbreviation of competition and enhancement.
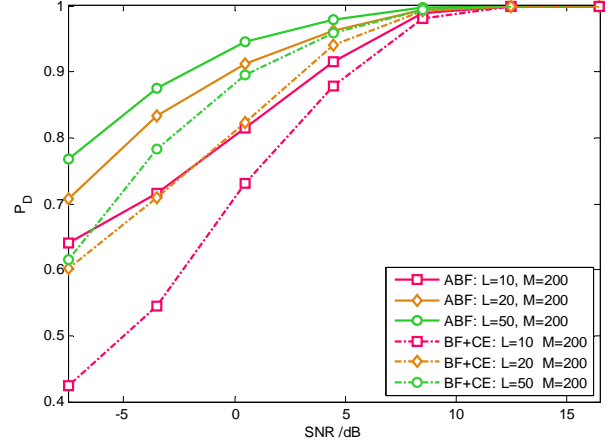

Fig. 9. Sensing performance of the new ABF scheme and others existing methods. Note that, here the BF scheme refers to the joint estimation and detection schemes developed in the previous works [12], [18].

Eq. (46) to simulate the dynamic switching of PUs' emission states, while in the estimation process we assume a simple yet inaccurate TPM, i.e. $\mathbf{P}$=[0.25 0.25 0.25 0.25; 0.25 0.25 0.25 0.25; 0.25 0.25 0.25 0.25; 0.25 0.25 0.25 0.25].

As expected, both the estimation MSE of unknown channel and the detection probability will be degraded. However, we found from Fig. 7 that the performance degradation is relatively slight, i.e., the estimation MSE was increased from 0.032 to 0.038 when SNR=12.5dB, and the detection accuracy was reduced from 0.9964 to 0.9956 when SNR is 8.5dB. Thus, we may conclude that our designed algorithm is immune to practical inaccurate information. The underlying reason may be that, when the SNR is relatively high, the likelihood would be accurate and the dependence on prior information of the recursive inference is alleviated. This is verified by the fact that, in low SNR regions (i.e. SNR<5dB), remarkable loss was observed from both estimation MSE and detection performance, e.g. the estimation MSE would be even increased from 0.3734 to 0.9068 (when SNR is -3.5dB for channel 2).

4) Comparative Analysis: Finally, we compare our designed ABF scheme with previous joint estimation methods (i.e. the classical BF algorithm) [12], whereby multiple TDD PUs in small cell are required to be detected/identified.

We firstly investigate the traditional BF scheme adopted by previous works [12], [40]. In a classical scheme, multiple separate chains may be employed to directly estimate total J PUs' occupancy states and track the trajectories of dynamic channels, where the *a priori* birth density of the jth PU may be evaluated via $p_j^b = \sum_{j' \neq j} p_{j' \to j}$. If the number of posterior existence densities surpassing a threshold (i.e., $q_{n|n,j} \geq \gamma$) is larger than 1, i.e. $|\mathcal{J}_n| \geqslant 1$, then we will reasonably infer that the jth PU with the maximum $q_{n|n,j}$ is most probably active, while the others remains inactive at each time n. It is noted that, unfortunately, any mechanisms in dealing with the indistinguishable problem are not embedded into classical BF methods [12], [18], [40]. There is also no additional post-processing (e.g. competitive and enhancement) to prevent the error propagation. As a consequence, it fails to accurately assess channel qualities and estimate multiple PUs' emission

states. From numerical results, the MSE of channel estimation will be 0.15 if an SNR is 16.5dB, when the sample size is M=200 and a static fading length is L=20, as in Fig. 8. By producing the high MSE and poor sensing performance, classical BF schemes can be hardly applied to shared access scenarios with multiple TDD PUs.

In order to alleviate the destructive influences from the unique indistinguishable problem and further enhance the estimation performance, another intuitive scheme is to combine the classical BF scheme with the proper post-processing methods. For example, we may integrate a competition and enhancement process into a classical BF method [12], [18]. From the numerical results in Fig. 8, by introducing the post-processing adjusting, the channel estimation MSE will be effectively reduced. Taking the 1st PU-SU link for example, by combining a classical BF with the competition and enhancement process, the MSE will be reduced from 0.15 to 0.012, under M=200 and L=20. Yet, since the sequential estimations of J chains are completely independent of each other, which can hardly take full advantage of the group transitional behaviors and the historical inference of existence densities, the acquired MSE performance seems still to be unsatisfied to practical applications.

From the comparative results in Fig. 8, with the designed ABF scheme the channel estimation performance can be improved significantly. Taking J=2 TDD PUs for example, the channel estimation MSE will be reduced to 4.5×10^{-3}, when the new ABF is applied to spectrum sensing with simultaneous channel qualities assessment. By utilizing the ABF scheme which fully takes the potential mutual interruptions and utilizes the group transitional property, the promising MSE performance will be attained, which could suppress the error propagation to the maximum.

Finally, we evaluate the sensing performance of the new ABF scheme. For the purpose of comparative analysis, we have plotted together the sensing performance of a classical BF scheme adopted by [12], which is further combined with our post-processing technique. From Fig. 9, the new ABF scheme will remarkably improve the sensing accuracy. For

example, when the right detection ratio P_D is about 0.9, a rough detection gain of 3dB can be obtained by the new ABF when the static channel length is configured to L=50, compared with a classical BF with additional post-processing. As shown by numerical results, our new ABF scheme may effectively cope with the indistinguishable problem when detecting multiple TDD PUs, which allows for the accurate assessment on dynamic channel qualities and obtain also the promising sensing performance.

Except for the improved channel utilization promoted by enhanced sensing accuracy, the estimated channel gains can be further utilized by shared users. For example, with the help of distributed accessing methods [29], [47], [48], the shared users can be now allowed to coexist in the occupied channel, by reconfiguring its emission power according to the tolerable interference at PU receiver. This further provides the great potential to future shared accessing by enabling the fine-grained resource sharing [46].

V. CONCLUSIONS

For the shared access in small-cell scenarios with multiple TDD users, identifying the active PU and estimating its associated link quality will be of great significance, which remains a formidable challenge. In this work, we structured it as a mixed classification and estimation (MCE) problem and designed a novel ABF algorithm, which accurately identifies the active PU and assess simultaneously the dynamic quality of all links. To implement this, a recursive multiple-chain estimation scheme is designed, and in each chain, the prediction and update procedure fully exploits the group transitional behavior and historical inference data. Furthermore, a competition and enhancement scheme is integrated to restrict the error propagation of this recursive method. Simulations are provided to validate the estimation performance of our ABF scheme in the context of multiple TDD PUs. Based on the numerical simulations, it is demonstrated that the new ABF algorithm can significantly enhance the detection/estimation performance. The resulting remarkable improvement on sensing accuracy can potentially contribute to the harmonious coexistence of shared access, and thereby facilitate the deployment of more flexible and efficient small-cell. E.g., except for the improved sensing accuracy, the estimated link quality further permits the deeper optimization of resources, by enabling more intelligent accessing and increased flexibility in spectrum reuse. Thus, the new sensing paradigm and the designed ABF algorithm will be of significance to future shared spectrum access.

APPENDIX A: DERIVATION OF PREDICTED EXISTENCE DENSITY

For each single-chain RFS, the jth predicted FISST PDF will be expanded into Eq. (A1). Considering the case of $\mathcal{F}_{n,j} \neq \varnothing$ (or $s_{n,j} = 1$), the predicted FISST can be further re-formatted to Eqs. (A2), see the bottom of the Page.

Further taking the 1-st order Markov model of transitional incumbent states, the predicted density of a NULL case (there is no active PU at time $n - 1$) is given by:

$$p_{n-1|n-1,j}(\varnothing|y_{1:n-1}) = \Pr\{s_{n-1,1} = 0, \cdots, s_{n-1,J} = 0\},$$
$$= \prod_{j=1}^{J}(1 - q_{n-1|n-1,j}). \quad (A3)$$

Similarly, the posterior density that there is only one active PU (e.g. the jth PU) is expressed as:

$$p_{n-1|n-1,j}(s_{n-1,j}|y_{1:n-1})$$
$$= \Pr\{s_{n-1,j} = 1, s_{n-1,j' \neq j} = 0\},$$
$$= q_{n-1|n-1,j} \times \prod_{j' \in \mathcal{J}, j' \neq j}(1 - q_{n-1|n-1,j'}). \quad (A4)$$

It is easily seen that the left of Eq. (A2) corresponds exactly to $q_{n|n-1,j}$. Substituting the above Eqs. (A3)-(A4) into (A2), the prediction existence density is then written as Eq. (21).

APPENDIX B: DERIVATION OF PREDICTED SPATIAL DENSITY

We still consider the case of $\mathcal{F}_{n,j} = \{h_{n,j}\}$. Relying on Eq. (A1), again this predicted FISST PDF will be re-formatted to Eq. (B1), see the Bottom of the next Page.

It is observed that, from the expanded Eq. (B1), the predicted posterior density involves also three components, i.e., the

$$p_{n|n-1,j}(\mathcal{F}_{n,j}|y_{1:n}) = \sum_{j'=1}^{J} \int \phi_{n|n-1}(\mathcal{F}_{n,j}|\mathcal{F}_{n,j'})p_{n-1|n-1,j'}(\mathcal{F}_{n-1,j'}|y_{1:n-1})\delta\mathcal{F}_{n-1,j'}, \quad (A1)$$

$$= \phi_{n|n-1}(\mathcal{F}_{n,j}|\varnothing)p_{n-1|n-1,j}(\varnothing|y_{1:n-1}) + \sum_{j'=1}^{J} \int \phi_{n|n-1}(\mathcal{F}_{n,j}|\mathcal{F}_{n-1,j'})p_{n-1|n-1,j'}(\mathcal{F}_{n-1,j'}|y_{1:n-1})\delta\mathcal{F}_{n-1,j'}.$$

$$p_{n|n-1,j}(s_{n,j} = 1|y_{1:n})$$

$$= p_{n|n-1,j}(s_{n,j} = 1|\varnothing)p_{n-1|n-1,j}(\varnothing|y_{1:n-1}) + \sum_{i=1}^{I} p_{n|n-1,j}(s_{n,j} = 1|s_{n-1,j'} = 1)p_{n-1|n-1,j'}(s_{n-1,j'} = 1|y_{1:n-1}).$$
$$(A2)$$

birth component $\mu^b_{n|n-1,j}(\{h_{n,j}\}|y_{1:n-1})$, the survival component $\mu^s_{n|n-1,j}(\{h_{n,j}\}|y_{1:n-1})$ and the transition component $\mu^s_{n|n-1,j}(\{h_{n,j}\}|y_{1:n-1})$.

For the predicted existence densities, the following equation holds for the jth RFS chain, i.e.

$$p_{n|n-1,j}(\{h_{n,j}\}|y_{1:n-1}) = \Pr(s_{n|n-1,j}=1) \times f_{n|n-1,j}(h_{n,j}). \tag{B2}$$

Given $\Pr(s_{n|n-1,j}=1) = q_{n|n-1,j}$ and with little manipulations, we will immediately have Eq. (22).

From Eq. (B1), the sub-component of birth is specified by:

$$\mu^b_{n|n-1,j}(\{h_{n,j}\}|y_{1:n-1})$$
$$\triangleq b_{n|n-1,j}(\{h_{n,j}\}) \times p_{n-1|n-1,j}(\varnothing|y_{1:n-1}), \tag{B3}$$

and where the predicted probability of a NULL case is given by previous Eq. (A3). After substituting the expression of Eqs. (A3) and (B3), we will obtain Eq. (23).

Then, the survival component $p^s_{n|n-1,j}(\{h_{n,j}\}|y_{1:n-1})$ and the transitional component $p^t_{n|n-1,j}(\{h_{n,j}\}|y_{1:n-1})$ are defined by Eqs. (B4) and (B5), respectively, see the Bottom of the Page. Similarly, the posterior density of time $(n-1)$ is expressed as:

$$p_{n-1|n-1,j}(\{h_{n-1,j}\}|y_{1:n-1})$$
$$= \Pr(s_{n-1|n-1,j}=1) \cdot f_{n-1|n-1,j}(h_{n-1,j}).$$

Given the prior transitional density $\phi_{n|n-1,j}(h_{n,j}|h_{n-1,j}) = \Theta_{k \to k',j}$, and further substituting Eq. (A4) into the survival/transition components of Eq. (B4) and (B5), we will obtain the expressions of Eqs. (24) and (25).

APPENDIX C: UPDATE OF PREDICTED DENSITIES

Now, we update the posterior existence density $q_{n|n,j}$ and the posterior spatial density $f_{n|n,j}(h_{n,j})$. Based on a Bayesian rule and new observations y_n, two posterior densities of

interest will be estimated recursively. To do so, we consider a special case $\boldsymbol{\mathcal{F}}_{n,j} = \varnothing$, thus the update equation will be:

$$p_{n|n,j}(\varnothing|y_{1:n-1}) = \frac{\varphi_n(y_n|\varnothing) \times p_{n|n-1,j}(\varnothing|y_{1:n-1})}{p(y_n|y_{1:n-1})}. \tag{C1}$$

As far as J separated chains are concerned, for each single chain the denominator will be simplified to:

$$p_j(y_n|y_{1:n-1}) = \varphi_n(y_n|\varnothing) \times \Pr(s_{n|n-1,j}=0)$$
$$+ \Pr(s_{n|n-1,j}=1) \times \int \varphi_n(y_n|h_{n,j}) f_{n|n-1,j}(h_{n,j}) dh_{n,j}. \tag{C2}$$

From a viewpoint of each RFS chain, we have $\Pr(s_{n|n-1,j}=0) = 1 - q_{n|n-1,j}$ and $\Pr(s_{n|n-1,j}=1) = q_{n|n-1,j}$. Relying on the previous Eqs. (C1) and (C2) as well as the underlying relationship $p_{n|n,j}(\varnothing|y_{1:n}) = 1 - q_{n|n,j}$, we will conveniently obtain the updated *a posteriori* existence density $q_{n|n,j}$ via the following relation:

$$1 - q_{n|n,j} = \varphi_n(y_n|\varnothing)(1 - q_{n|n-1,j})/\Big\{ \varphi_n(y_n|\varnothing)(1 - q_{n|n-1,j})$$
$$+ q_{n|n-1,j} \int \varphi_n(y_n|h_{n,j}) f_{n|n-1,j}(h_{n,j}) dh_{n,j} \Big\}. \tag{C3}$$

For clarity, the likelihood ratio of two hypothesis (i.e. the presence and absence of the jth PU) conditioned on the jth channel state $h_{n,j}$ is denoted by:

$$r_{n,j}(y_n|\{h_{n,j}\}) \triangleq \varphi_n(y_n|h_{n,j})/\varphi_n(y_n\varnothing). \tag{C4}$$

Replacing the expression of Eq. (C2) into Eq. (C3), $q_{n|n,j}$ will be finally derived via Eq. (26).

Then, considering the other case of $\boldsymbol{\mathcal{F}}_{n,j} = \{h_{n,j}\}$, the identity relation $p_{n|n,j}(\{h_{n,j}\}|y_{1:n}) = q_{n|n,j} \times f_{n|n,j}(h_{n,j})$ will hold similarly. Further taking the derived $q_{n|n,j}$ in Eq. (26), we can update $f_{n|n,j}(h_{n,j})$ via Eq. (27).

$$p_{n|n-1,j}(\{h_{n,j}\}|y_{1:n-1})$$
$$= \phi_{n|n-1,j}(\{h_{n,j}\}|\varnothing) \cdot p_{n-1|n-1,j}(\varnothing|y_{1:n-1}) + \sum_{j' \in \mathcal{J}} \int_{\mathcal{H}_{j'}} \phi_{n|n-1,j}(h_{n,j}|h_{n-1,j'}) \cdot p_{n-1|n-1,j}(\{h_{n-1,j'}\}|y_{1:n-1}) dh_{n-1,j'},$$
$$= b_{n|n-1,j}(\{h_{n,j}\}) \cdot p_{n-1|n-1,j}(\varnothing|y_{1:n-1}) + \int_{\mathcal{H}_j} \phi_{n|n-1,j}(h_{n,j}|h_{n-1,j}) \cdot p_{n-1|n-1,j}(\{h_{n-1,j}\}|y_{1:n-1}) dh_{n-1,j}$$
$$+ \sum_{j' \neq j} \int_{\mathcal{H}_{j'}} p_{j' \to j} \times b_{n|n-1,j}(h_{n,j}) \cdot p_{n-1|n-1,j'}(\{h_{n-1,j'}\}|y_{1:n-1}) dh_{n-1,j'}. \tag{B1}$$

$$\mu^s_{n|n-1,j}(\{h_{n,j}\}|y_{1:n-1}) \triangleq \int_{\mathcal{H}_j} \phi_{n|n-1,j}(h_{n,j}|h_{n-1,j}) \cdot p_{n-1|n-1,j}(\{h_{n-1,j}\}|y_{1:n-1}) dh_{n-1,j}. \tag{B4}$$

$$\mu^t_{n|n-1,j}(\{h_{n,j}\}|y_{1:n-1}) \triangleq \sum_{j' \neq j} \int_{\mathcal{H}_{j'}} p_{j' \to j} \times b_{n|n-1,j}(h_{n,j}) \cdot p_{n-1|n-1,j'}(\{h_{n-1,j'}\}|y_{1:n-1}) dh_{n-1,j'},$$
$$= b_{n|n-1,j}(h_{n,j}) \times \sum_{j' \neq j} \int_{\mathcal{H}_{j'}} p_{j' \to j} \cdot p_{n-1|n-1,j'}(s_{n-1,j'}=1|y_{1:n-1}) dh_{n-1,j'}. \tag{B5}$$

$$w_{n|n-1,j}^{(i)} =$$

$$
\begin{cases}
\dfrac{p_{n,j}^s \cdot q_{n-1|n-1,j} \prod_{j' \neq j}(1 - q_{n-1|n-1,j'})}{q_{n|n-1,j}} \times \dfrac{\Theta\left(x_{n|n-1}^{(i)}\big|x_{n-1|n-1}^{(i)}\right)}{\xi_{n,j}\left(x_n|x_{n-1}^{(i)}, y_{1:n}\right)} \times w_{n-1|n-1}^{(i)}, & i = 1, 2, \cdots, N, \quad \text{(D3-a)} \\[4ex]
\dfrac{p_{n,j}^b \prod_j (1 - q_{n-1|n-1,j}) + p_{j' \to j} \sum_{j' \neq j} q_{n-1|n-1,j'} \prod_{j'' \neq j'} (1 - q_{n-1|n-1,j''})}{q_{n|n-1}} \cdot \dfrac{b_{n|n-1}\left(x_{n|n-1}^{(i)}\right)}{B\beta_{n,j}(x_n|y_{1:n})}, & i = N+1, \cdots, N+B. \quad \text{(D3-b)}
\end{cases}
$$

APPENDIX D: IMPLEMENTATION OF PF

In principle, PF employs a group of random discrete particles $x^{(i)}$ to approximate the non-analytical PDF, e.g. the predicted spatial density $f_{n|n-1,j}(h_{n,j})$. Such simulated particles are attached also with the evolving probability masses (or weights) $w^{(i)}$ ($i = 1, 2, \cdots, I$).

PF consists of two recursive operations [41], [42], i.e., (1) sequential importance sampling and (2) weights updating. First, I particles are simulated from a proposal distribution (or importance function) $\pi(x_n|x_{1:n-1}, y_{1:n})$, i.e., $x_n^{(i)} \sim \pi(x_n|x_{1:n-1}, y_{1:n})$. Second, the importance weights $w_n^{(i)}$ are updated via:

$$w_n^{(i)} = w_{n-1}^{(i)} \times \frac{p\left(y_n|x_n^{(i)}\right) \cdot p\left(x_n^{(i)}|x_{n-1}^{(i)}\right)}{\pi(x_n|x_{1:n-1}, y_{1:n})}. \quad \text{(D1)}$$

Then, the particle weights will be normalized to 1, i.e., $w_n^{(i)} = w_n^{(i)} / \sum_i w_n^{(i)}$. In practice, a re-sample process is used to discard particles of negligible weights [42].

PF Implementations: In order to approximate the predicted spatial density via $f_{n-1|n-1}(x) = \sum_{i=0}^{I-1} w_{n|n-1}^{(i)} \times \delta\left(x - x_{n|n-1}^{(i)}\right)$ [12], [40], total $(N + B)$ discrete particles will be simulated from the proposal distribution, as in Eq. (D2). Here, the proposal density is piece-wise, since the spatial density $f_{n|n-1}(x)$ in the Eq. (22) involves multiple components. To be specific, the first N particles correspond to the survival component, while the following B particles will approximate the birth/traditional component, i.e.,

$$x_{n|n-1}^{(i)} \sim \begin{cases} \xi_{n,j}\left(x_n|x_{n-1}^{(i)}, y_{1:n}\right), & i = 1, 2, \cdots, N, \quad \text{(D2-a)} \\ \beta_{n,j}(x_n|y_{1:n}), & i = N+1, \cdots, N+B. \quad \text{(D2-b)} \end{cases}$$

Replacing the related densities into above Eq. (D1), the associated weights will be updated via Eq. (D3), see the Bottom of the page.

Proposal Densities: The birth density and the other survival density in Eq. (D2) are of great importance, which shall be properly designed.

For the birth component, we suggest an adaptive density by fully exploiting the MAP estimation of time $(n-1)$ as well as the *a priori* transitional densities of fading channels. For the time $(n-1)$, denote the estimated channel state of the jth PU with $\hat{h}_{n-1,j}$, i.e., $\hat{h}_{n-1,j} = \arg \max_{h_{n-1,j} \in \mathcal{H}_j} f_{n-1|n-1,j}(h_{n-1,j})$. First, we expand this single state $\hat{h}_{n-1,j}$ to a small set $\mathcal{H}'_{n|n-1,j}$ by increasing the estimation diversity, i.e.,

$$\mathcal{H}'_{n|n-1,j} \triangleq \{h_{n-1,j} = \mathsf{H}_{k,j} | \hat{h}_{n-1,j} = \mathsf{H}_{k',j}, |k - k'| \leq 1\},$$

and then, each states in $\mathcal{H}'_{n-1,j}$ will transit to one feasible subsequent state according to the prior TPM Θ_j. By doing so, a group of new birthed particles of time n will be derived.

For the survival density $\xi_n\left(x_n|x_{n-1}^{(i)}, y_{1:n}\right)$, we use directly the posterior density of time $(n-1)$ [16]. With the new particle weights $\left\{x_{n-1|n-1}^{(i)}, w_{n-1|n-1}^{(i)}\right\}_{i=0}^{I-1}$, the posterior density of time $(n-1)$ will be estimated, via which N particles are simulated. Thereafter, such N particles will be survived to time n.

REFERENCES

[1] J. G. Andrews, S. Buzzi, W. Choi, et al. "What will 5G be?" *IEEE Journal on Selected Areas in Communications*, vol. 32, no. 4, pp. 1065-1082, 2014.

[2] C. X. Wang, F. Haider, X. Gao, et al. "Cellular architecture and key technologies for 5G wireless communication networks," *IEEE Communications Magazine*, vol. 52, no. 2, pp. 122-130, 2014.

[3] M. Mueck, W. Jiang, G. L. Sun, H, W, Cao, E. Dutkiewicz, S. Choi, *White Paper: Novel Spectrum Usage Paradigms for 5G*, IEEE Technical Committee on Cognitive Networks SIG CR in 5G, Nov., 2014.

[4] A. Al-Dulaimi, S. Al-Rubaye, Q. Ni, et al. "5G communications race: pursuit of more capacity triggers LTE in unlicensed band," *IEEE Vehicular Technology Magazine*, vol. 10, no. 1, pp. 43-51, 2015.

[5] N. Rupasinghe, I. Guvenc. "Licensed-assisted access for WiFi-LTE coexistence in the unlicensed spectrum," *in Proc. Of IEEE Globecom Workshops (GC Wkshps)*, pp. 894-899, 2014.

[6] H. J. Zhang, X. Chu, W. Guo, and S. Wang, "Coexistence of Wi-Fi and Heterogeneous Small Cell Networks Sharing Unlicensed Spectrum," *IEEE Communications Magazine*, vol. 53, no. 3, pp. 158-164, 2015.

[7] D. Catania, M. G. Sarret, A. F. Cattoni, et al, "Flexible UL/DL in Small Cell TDD Systems: A Performance Study with TCP Traffic," in Proc. of *IEEE vehicular technology conference* (VTC) pp. 1-6, 2015,.

[8] Y.-C. Liang, K. C. Chen, G. Y. Li, and P. Mähönen, "Cognitive radio networking and communications: an overview," *IEEE Transactions on Vehicular Technology,* vol. 60, no. 7, pp. 3386-3407, 2014.

[9] X. Kang, Y. C. Liang, H. K. Garg, et.al, "Sensing-based spectrum sharing in cognitive radio networks," *IEEE Transactions on Vehicular Technology,* vol. 58, no. 8, pp. 4649-4654, 2009.

[10] L. B. Le, E. Hossain, "Resource allocation for spectrum underlay in cognitive radio networks," *IEEE Transactions on Wireless Communications*, vol. 7, no. 12, pp. 5306-5315, 2008.

[11] Yuhua Xu, Jinlong Wang, Qihui Wu, Zhiyong Du, Liang Shen and Alagan Anpalagan, "A game theoretic perspective on self-organizing optimization for cognitive small cells," *IEEE Communications Magazine*, vol. 53, no. 7, pp.100-108, 2015.

[12] B. Li, S. H. Li, Y. J. Nan, A. Nallanathan, C. L. Zhao, Z. Zhou "Deep Sensing for Next-generation Dynamic Spectrum Sharing: More Than Detecting the Occupancy State of Primary Spectrum," *IEEE Transactions on Communications*, vol. 63, no. 7, pp. 2442-2457, 2015.

[13] Q. Zhao, B. M. Sadler, "A survey of dynamic spectrum access," *IEEE Signal Processing Magazine*, vol. 24, no. 3, pp. 79-89, 2007.

[14] Y.-C. Liang, A. T. Hoang, and H. H. Chen, "Cognitive radio on TV bands: A new approach to provide wireless connectivity for rural areas," *IEEE Wireless Commun.,* vol. 15, no. 3, pp. 16-20, 2008.

[15] Z. Lei, S. J. Shellhammer, "IEEE 802.22: The first cognitive radio wireless regional area network standard," *IEEE communications magazine*, vol. 15, no. 3, pp. 130-138, 2009.

[16] F. F. Gao, K. Q. Zhang, "Enhanced Multi-Parameter Cognitive Architecture for Future Wireless Communications," *IEEE Communications Magazine*, vol. 53, no. 7, pp. 86-92, 2015.

[17] F. F. Gao, J. C. Li, T. Jiang, and W. Chen, "Sensing and Recognition When Primary User Has Multiple Transmit Power Levels," *IEEE Transactions on Signal Processing*, vol. 63, no. 10, pp. 2704-2717, 2015.

[18] B. Li, S. H. Li, A. Nallanathan, C. L. Zhao, "Deep Sensing for Future Spectrum and Location Awareness 5G Communications," *IEEE Journal Selected Areas Communications*, vol. 33, no. 7, pp. 1331-1344, 2015.

[19] J. Ma, G. Y. Li, and B. H. Juang, "Signal Processing in Cognitive Radio," *The Proceedings of IEEE*, vol. 97, no. 5, pp. 805-823, 2009.

[20] E. Axell, G. Leus, E. G. Larsson, and H. V. Poor, "Spectrum Sensing for Cognitive Radio: State-of-the-art and recent advances," *IEEE Signal Processing Magazine*, vol. 29, no. 3, pp. 101-116, 2012.

[21] F. F. Digham, M. S. Alouini, and M. K. Simon, "On the Energy Detection of Unknown Signals Over Fading Channels," in Proc. of *IEEE international Conference on Communications (ICC)*, Anchorage, AK, vol. 5, pp. 3575-3579, 2003.

[22] R. Tandra and A. Sahai, "SNR walls for signal detection," *IEEE J. Sel. Topics Signal Process.*, vol. 2, no. 1, pp. 4-17, 2008.

[23] D. Cabric, S. M. Mishra, R. M. Brodersen, "Implementation issues in spectrum sensing for cognitive radios," *in Proc. of* the Thirty-Eighth Asilomar Conference on Signals, Systems and Computers, pp. 772-776, 2004.

[24] J. Lundén, V. Koivunen, A. Huttunen, and H. V. Poor, "Spectrum sensing in cognitive radios based on multiple cyclic frequencies," *in Proc. of* IEEE Int. Conf. Cognitive Radio Oriented Wireless Networks and Commun. (Crowncom), Orlando, Florida, USA, July.2007.

[25] B. Li, C. L. Zhao, M. W. Sun, Z. Zhou, A. Nallanathan, "Spectrum Sensing for Cognitive Radios in Time-Variant Flat Fading Channels: A Joint Estimation Approach," *IEEE Transactions on Communications*, vol. 62, no. 8, pp. 2665-2680, 2014.

[26] K. Paul, A. Varghese, S. Iyer, et al. "WiFiRe: rural area broadband access using the WiFi PHY and a multisector TDD MAC," *IEEE Communications Magazine*, vol. 45, no. 1, pp. 111-119, 2007.

[27] T. Nakamura, S. Nagata, A. Benjebbour, "Trends in small cell enhancements in LTE advanced," *IEEE Communications Magazine*, vol. 51, no. 2, pp. 98-105, 2013.

[28] H. Ishii, Y. Kishiyama, and H. Takahashi, "A novel architecture for LTE-B: C-plane/U-plane split and phantom cell concept," *in Proc. Int. Workshop Emerging Technol. LTE-Adv. Beyond-4G* Conjunction GLOBECOM, Anaheim, CA, USA, Dec. 3C7, pp. 624-630, 2012.

[29] Y. Xing, C. N. Mathur, M. A. Haleem, R. Chandramouli, K. P. Subbalakshmi, "Dynamic spectrum access with QoS and interference temperature constraints," *IEEE Transactions on Mobile Computing,* vol. 6, no. 4, pp.423-433, 2007.

[30] B. Vujitic, N Cackov, S. Vujitic. "Modeling and characterization of traffic in public safety wireless network," in Proc. of *Int. Symp. Performance Evaluation of Computer and Telecommunication Systems*, Edinburgh, UK, pp. 213-223, 2005.

[31] P. Sadeghi, R. Kennedy, P. Rapajic, R. Shams, "Finite-state Markov Modeling of Fading Channels: A Survey of Principles and Applications," *IEEE Signal Processing Magazine*, vol. 25, no. 5, pp. 57-80, 2008.

[32] H. S. Wang, N. Moayeri, "Finite-state Markov Channel: A Useful Model for Radio Communication Channels," *IEEE Transactions on Vehicular Technology,* vol. 44, no. 1, pp. 163-171, 1995.

[33] H. S. Wang, P. Chang, "On Verifying the First Order Markovian Assumption for A Rayleigh Fading Channel Model," *IEEE Transactions on Vehicular Technology,* vol. 45, no. 2, pp. 353-357, 1996.

[34] G. Breit, H. Sampath, S. Vermani, et.al. "TGac Channel Model Addendum," IEEE802.11-09/0308r12, 2010.

[35] Y. C. Liang, Y. H. Zeng, E. C. Y. Peh, et al. "Sensing-throughput tradeoff for cognitive radio networks," *IEEE Transactions on Wireless Communications*, vol. 7, no. 4, pp. 1326-1337, 2008.

[36] Y. H. Zeng, Y. C. Liang, "Eigenvalue-based Spectrum Sensing Algorithms for Cognitive Radio," *IEEE Trans Commun.*, vol. 57, no. 6, pp. 1784C1793, 2009.

[37] R. Mahler, *Statistical Multisource Multitarget Information Fusion*. Norwood, MA, USA: Artech House, 2007.

[38] B.-T. Vo and B.-N. Vo, "A Random Finite Set Conjugate Prior and Application to Multi-target Tracking," in Proc.*7th IEEE Int. Conf. Intell. Sens., Sens. Netw. Inf. Proc. (ISSNIP)*, Adelaide, Australia, pp. 431-436, 2011.

[39] B.-T. Vo, B.-N. Vo, and A. Cantoni, "Bayesian filtering with random finite set observations," *IEEE Trans. Signal Process.*, vol. 56, no. 4, pp. 1313-1326, 2008.

[40] B. Ristic, Ba-Tuong Vo, Ba-Ngu Vo, A. Farina, "A Tutorial on Bernoulli Filters: Theory, Implementation and Applications," *IEEE Trans. Signal Process.*, vol. 61, no. 13, pp. 3406-3430, 2013.

[41] P. M. Djuric, J. H. Kotecha, J. Q Zhang, Y. F. Huang, T. Ghirmai, M. F. Bugallo, J. Miguez, "Particle filtering," *IEEE Signal Processing Magazine*, vol. 20, no. 5, pp. 19-38, 2003.

[42] A. Doucet, S. Godsill, C. Andrieu, "On sequential Monte Carlo sampling methods for Bayesian filtering," *Statistics and computing*, vol. 10, no. 3, pp. 197-208, 2000.

[43] Zheng S, P. Y. Kam, Y. C. Liang, et al., "Spectrum Sensing for Digital Primary Signals in Cognitive Radio: A Bayesian Approach for Maximizing Spectrum Utilization," *IEEE Transactions on Wireless Communications*, vol. 12, no. 4, pp. 1774-1782, 2013.

[44] Q. Q. Liang, M. Y. Liu, D. F. Yuan, "Channel estimation for opportunistic spectrum access: uniform and random sensing," *IEEE Trans. on Mobile Computing*, vol. 11, no. 8, pp. 1304-1316, 2011.

[45] I. Siekmann, W. L. Nd, D. Yule, et al., "MCMC Estimation of Markov Models for Ion Channels," *Biophysical Journal*, vol. 100, no. 8, pp. 1919-1929, 2011.

[46] M. G. Khoshkholgh, K. Navaie, H. Yanikomeroglu, "Access strategies for spectrum sharing in fading environment: overlay, underlay, and mixed," *IEEE Transactions on Mobile Computing*, vol. 9, no. 12, pp. 1780-1793, 2010.

[47] D. Niyato, E. Hossain, "Competitive Pricing for Spectrum Sharing in Cognitive Radio Networks: Dynamic Game, Inefficiency of Nash Equilibrium, and Collusion," *IEEE Journal on Selected Areas in Communications*, vol. 26, no.1, pp.192-202, 2008.

[48] C. Q. Fan, B. Li, C. L. Zhao, et al., "Learning-based Spectrum Sharing and Spatial Reuse in mm-Wave Ultra Dense Networks," *IEEE Transactions on Vehicular Technology*, doi:10.1109/TVT.2017.2750801, pp. 1-15, 2017.